ADAPTIVE DIGITAL SONAR BEAMFORMING: A SIMULATED HARDWARE RESPONSE TO WEAK SIGNALS

M. TRIVEDI

Marconi Underwater Systems Ltd., Elettra Avenue, Waterlooville, Hampshire, England.

1 INTRODUCTION

The problem of removing spatial narrow/broadband interferences from sonar beams has long been described in the subject literature. A plethura of adaptive beamforming techniques has been published over the past couple of decades. Adaptive beamforming techniques are useful when weak signals are to be detected in the presence of strong interferers, Winder [1].

The advantage of using adaptive methods over the conventional approach when beamforming with a short array (eg. 8 elements) is obvious. Here, the resolution of a weak target signal can be enhanced by suppressing unwanted strong sources residing within the relatively broad main-lobe response by developing nulls in such directions, see Smith [2]. In the case of beamforming with longer arrays the need for employing adaptive techniques is less obvious since a relatively narrow main-lobe makes it less likely for a weak signal to be masked by the presence of a nearby interferer. Moreover, interferers lying within the now lower (but more extensive) sidelobe structure can be suppressed further by simply shading the array elements.

However, the width of the array's main-lobe is inversely proportional to signal frequency and the effective array aperture in the specified 'look' direction. Shading the array, as is usual, will broaden the main-lobe response further. It is easy to appreciate why adaptive methods can provide an overall more effective rejection of interferers, lying within or very close to the main-lobe, even when beamforming using longer arrays.

Moreover, as shown here and elsewhere, Trivedi & Atmore [3], adaptive beamforming can enhance signal detectability when interferers reside in the array side-lobes, at least in the case of a medium sized (32-element) linear array. By steer nulls of adequate depth and width automatically in such directions, it is possible to achieve a greater suppression of these undesired sources than can be achieved by a simple shading of the array elements. This is especially true in the presence of noise, gain and phase mismatches between the array hydrophones.

1.1 The Aim of the Paper

In this paper the enhanced detectability of weak signals achieved by adaptive methods over the conventional beamforming approach is demonstrated. This is illustrated through simulated scenarios deploying strong, spatially separated broadband interferers. The benefits of adaptive beamforming are illustrated via the well known Frost technique incorporating zero and first–order derivative gain constraints. This type of adaptive beamforming is equivalent to the Generalised Sidelobe Canceller (GSC) approach of Buckley & Griffiths [4]. The use of array shading within the adaptive process is shown to improve the interference rejection performance of the beamformer in the side-lobe regions when using a medium sized (eg. 32-element) linear array. This aspect of adaptive beamforming appears not to have been addressed in the subject literature in any great detail.

The above beamforming aspects are demonstrated through the use of Fortran based simulations written to evaluate the hardware performance of a single-card implementation of an adaptive digital sonar beamformer reported by Trivedi et al [5]. Hardware execution benchmarks for the implemented Frost algorithm and its variants such as Duvall and the GSC method are presented. The effects of noise, gain and phase mismatches between the array elements on signal detectability using an equi-spaced, 32-element linear array are also presented. The Least Mean Squares (LMS) based Frost beamforming approach is adopted in this paper since it is simpler and faster to compute than the optimal Exact Least Squares (ELS) approach which requires matrix inversions, see [5].

2 ADAPTIVE ARRAY PROCESSING

The block diagram of the adaptive array processing described in [5] is shown in Fig.1. Beam steering is achieved by inserting inter-element broadband time delays appropriate to the array geometry and the specified 'look' direction. If desired, the array elements may be shaded prior to the adaptive beamforming process. The hardware implementation of the adaptive beamformer outlined in [5] is shown schematically in Fig.2. All simulated scenarios, with or without array shading, are generated to 16-bit (2's complement) accuracy and applied as real array samples, X(k), see Fig.2. The adaptively updated (real) filter weights, W(k), are computed to single-precision, floating-point accuracy by the TMS320C30 DSP chip, see Fig.2. These weights are converted to 16-bit integer values (by the DSP chip) and applied to the 16-bit array samples (X(k)) via a 16x16 bit Multiplier-Accummulator (MAC) chip. The resulting 31-bit adaptively filtered (ie. spatially beamformed) MAC output is truncated to a 16-bit temporal output (y(k) in Figs.1 & 2). This k^{th} output is also used in the LMS weight update process as detailed in section 2.2.

2.1 Frost Beamforming

The Frost approach, see Frost [6], is conceptually simple and computationally easy to implement. The broadband signal gain in the 'look' direction is constrained to unity while plane interference wavefronts arriving from any other direction (and contributing as side-lobe leakages) are minimised in the LMS sense.

2.1.1 Steering Direction Considerations

Without higher Order Gain Constraints (OGC) the Frost beam response can be very narrow about the 'look' direction. Unless the desired signal is perfectly aligned with the steered 'look' direction the pencil-sharp adaptive response can remove the signal from the beam, eventually, see [3]. The rate of removal of the misaligned signal accentuates as the input Signal-to-Interference-Noise-Ratio (SINR) at the array elements increases and the beam width decreases, Hudson [7]. Furthermore, since the gain is constrained to unity in the 'look' direction only, the beamformer can develop higher gains in other directions thereby, enhancing any noise present. This is especially true of directions close to the 'look' direction when the beamformer weights can get large while attempting to null the misaligned signal. The effect of including a first order derivative constraint is to broaden the beam response about the 0 degree 'look' direction, see [3]. Signals arriving from within a degree of the 'look' direction (for a K=32 element linear array) are passed without suffering significant long-term attenuation. In high SINR conditions a narrow main-lobe response results. In practice, the presence of strong interferers and noise at the array elements will broaden the main-lobe response. The topic of derivative gain constraints in dealt with in greater detail in section 2.2.1.

In this paper, direction misalignment errors of upto 5 degrees about the 'look' direction have been simulated for a 32-element array for low input SINRs (-30 dB) at the array elements. The inclusion of first order (derivative) gain constraint was found to have an insignificant effect on such misaligned 'look' signals. However, under high SINR conditions (eg. +10 dB) even the inclusion of first order constraint can not prevent the signal from being nulled with time, if it is misaligned by more than a few degrees about the 'look' direction, see [3]. The above comments also apply to continuous and pulsed signals of long duration in 'off-look' directions under low SINR conditions, though the rate of signal nulling is very much reduced. Nevertheless, inclusion of first order (derivative) gain constraint can be beneficial in practice, even though the input SINR can vary widely. Such an inclusion can reduce the number of beams required to cover a specified volume of space by broadening the individual beams, especially under high SINR conditions. Higher order derivative constraints may be used to broaden the beam further at the expense of the available degrees of freedom and increased computational load, Er and Cantoni [8]. Alternatively, a combination of few, lower order constraints and a weight-norm constraint on the beamformer weights [7] may be used to broaden the beam about the 'look' direction. The weight-norm technique, which is readily applicable to Frost type of beamformers (via the 'scaled projection' method), Cox et al [9], effectively limits the noise gain about the 'look' direction in high SINR scenarios.

2.1.2 Signal-Interference-Coherency Considerations

When a significant degree of spectral overlap exists between the 'look' direction signal and the other spatially separated sources beamforming based on a power minimisation criterion (e.g. Frost, GSC & ELS) cannot distinguish between the received coherent components. Thus, in nulling the interference, the beamformer can also, inadvertently, cancel a part (or even all) of the 'look' signal in the process of minimising the total power at its output. This loss in the desired signal due to Coherent-Signal-Cancellation (CSC) effects can occur in spite of the constant gain constraint applied in the 'look' direction. For example, the Frost beamformed continuous wave (CW) signal pulse in Fig.6 exhibits 'gashes' in its envelope as a result of CSC effects. Here, a weak signal pulse (-30 dB

relative to the total interference power) is detected in the presence of four (+24 dB) broadband interferers the frequency bands of which overlap with that of the pulsed CW tonal signal.

One approach is to isolate the 'look' direction signal from the power minimisation process by employing a 'master-slave' Frost beamformer configuration as proposed by Duvall, Duvall [10]. This achieved by a simple differencing between pairs of consecutive array elements prior to input to the 'master' Frost beamformer, also see [3]. The resulting Duvall beam response which is much broader than the corresponding Frost response, see [3], is therefore, less susceptible to steering misalignment errors. However, the application of the Duvall technique beside being limited mainly to a linear, equi-spaced array configuration is also very prone to noise, gain and phase mismatch errors between the array elements, see [3]. Other ways of overcoming CSC effects employ some form of spatial smoothing of the sensor data in order to 'breakup' the correlation existing between the 'look' signal and the interferers. One of these methods uses a number of Frost sub-beamformers each sharing a number of overlapping array elements with its neighbours, see Su et al [11]. Variations of the above based on the ELS and Recursive Least Squares (RLS) approaches use smoothed estimates of the spatial covariance matrix, see Shan & Kailath [12, 13] and Lee and Wu [14]. These alternative approaches appear to be computationally more demanding and cumbersome to implement than the constrained shaded Frost/GSC LMS approach considered in this paper.

In this paper the issue of Coherent-Signal-Cancellation (CSC) is addressed by incorporating array shading within the Frost beamforming process. In the case of an unshaded linear array the Frost beamformer weights evolve in response to a '*sin(x)/x*' acoustic beam pattern which exhibits large side-lobes. The use of a non-uniform array shading reduces the otherwise large leakage of the interferers when residing in the side-lobe regions. This leakage reduction mitigates the extent of cancellation suffered by a spectrally coherent 'look' signal and also leads to other beneficial effects outlined later on. The effects of array shading on the adaptive response close to the main-lobe region is addressed in section 4.2. Before presenting algorithm benchmarks and hardware simulation results, the iterative weight update process for the constrained Frost LMS beamforming is outlined.

2.2 Weight Generation Scheme

The Frost approach employs a linearly constrained, gradient descent, power minimisation algorithm. The Frost beamformer weights, W(k+1), are generated iteratively from W(k), see, [3, 4 & 6]:

$$W(k+1) = P.\{W(k) - \mu.y(k).X(k)\} + FF \quad \ldots\ldots(1)$$

where, $FF = W(0) = C.(C^T.C)^{-1}.FV$ denotes the initial weights with FV as the (L.Jx1) 'look' direction frequency response constraint vector. The integer L depends on the number and the nature of constraints employed as well as the array geometry. 'μ' is the convergence factor controlling the trade off between rate of convergence and misadjustment noise [3]. 'μ' can be held constant or updated adaptively (for example, see, Bragard and Jourdain [15]). C is the (K.JxL.J) broadband directional gain constraint matrix with its transpose C^T satisfying the 'look' direction gain constraint $C^T.W = FV$. K denotes the number of array elements and J is the number of taps per element. The k^{th} beamformed Frost output y(k) is formed by weighting the elements of the (K.Jx1) data column vector X(k) snapshot by the (K.Jx1) weight vector W(k). The vector X(k) is depicted in Figs.1 & 2 as a KxJ matrix held within the forward-path transversal (eg. FIR) filter structure. The matrix P is referred to as the projection matrix which is defined as:

$$P = I - C.(C^T.C)^{-1}.C^T \quad \ldots\ldots(2)$$

where, in Eqn(2) 'I' is a K.JxK.J matrix with unity diagonal elements. In case of a Frost algorithm with only a 0 OGC, L = 1 with C as a K.JxJ matrix. J degrees of freedom are lost in the case of a linear array. For a Frost with 0+1 OGC, L = 2 with C now as a K.Jx2.J matrix. For a linear array, 2.J degrees of freedom are lost [8].

2.2.1 Array Shading & First Order Gain Constraint

A direct implementation of the GSC approach results in a simpler unconstrained LMS weight update algorithm, see [4, 5]. However, such an approach requires a number of operations, such as the application of the signal blocking matrix and the generation of the (shaded) reference beam, to be implemented in hardware, elsewhere, see [5]. In this paper however, the above operations will be carried out in software as part of the weight update process. This is achieved by modifying the zero-order Frost 'look' gain constraint to cater for the amplitude modulation at the elements due to array shading and by introducing a first-order (derivative) gain constraint within the Frost algorithm, as outlined below. This alternative approach is shown to be equivalent to the GSC approach, see Eqn (14) of [4].

In the original Frost paper [6] the filter data, X(k), and the weight coefficients, W(k), were treated as K.Jx1 vectors. However, for notational convenience X(k) and W(k) are treated as KxJ matrices in the following expressions.

Let s(i), (i=1, 2....K) denote the symmetrical set of array shading coefficients. Let c(i), (i = 1, 2,....K) denote the antisymmetrical set of first order derivative gain constraint coefficients for an equispaced, linear K-element array for a given 'look' direction. The array mid-point is selected as a zero phase centre. For a derivation of c(i)s, refer to [8]. By incorporating terms s(i) and c(i) within matrix 'C' in Eqn (2) it can be shown that Eqn (1) can be expressed in its algorithmic form where the $(k+1)^{th}$ weight element is given iteratively in terms of the k^{th} weight, w(k,i,j), by:

$$w(k+1,i,j) = TERM(i,j) - s(i).SUM0(j) - c(i).SUM1(j) + g(i,j) \quad \ldots\ldots(3)$$

where, i is the row index (= 1, 2,...K is the number of array elements) and j is the column index (= 1, 2,...J is the number of taps per element) of the KxJ matrix, and where,

$$TERM(i,j) = w(k,i,j) - \mu.y(k).x(k,i,j) \quad \ldots\ldots(4)$$

$$SUM0(j) = \frac{1}{SSQ}.\sum_{n=1}^{K} s(n).TERM(n,j) \quad \ldots\ldots(5)$$

$$SUM1(j) = \frac{1}{CSQ}.\sum_{n=1}^{K} c(n).TERM(n,j) \quad \ldots\ldots(6)$$

$$SSQ = \sum_{m=1}^{K} s(m)^2 \quad \ldots\ldots(7)$$

$$CSQ = \sum_{m=1}^{K} c(m)^2 \quad \ldots\ldots(8)$$

$$g(i,j) = \frac{s(i).f(j)}{SSQ} \quad \ldots\ldots(9)$$

where, n and m are dummy row indices (= 1, 2,...K), and

$$f(j) = \begin{cases} 1 & j = \text{Integer}\left[\frac{J+1}{2}\right] \\ 0 & j \neq \text{Integer}\left[\frac{J+1}{2}\right] \end{cases} \quad \ldots\ldots(10)$$

f(j) is the composite gain constraint (Jx1) column vector for 'look' direction signals. In Eqn (10) an "all-pass" unity column gain response {eg. 0,..1,..0} has been used. However, a different frequency response could have been specified, instead. In the case of uniform array shading (ie. s(i)s all equal unity) and a zero order only gain constraint (ie. c(i)s all zeros) Eqn (3) reduces to the following familiar form proposed by Frost in his original paper, see page 930 of [6];

$$w(k+1,i,j) = TERM(i,j) - \frac{1}{K}.\sum_{n=1}^{K} TERM(n,j) + \frac{f(j)}{K} \quad \ldots\ldots(11)$$

An important point to note is that for non-uniform shading functions the equivalent Frost signal gain in the 'look' direction is given by;

$$FRSTLKSG = \sum_{i=1}^{K} g(i,M) = \frac{1}{SSQ}.\sum_{i=1}^{K} s(i) \quad \ldots\ldots(12)$$

where, $M = Int[(J+1)/2]_{th}$. column for which f(j) = 1 in Eqn (10) and zero for other columns. FRSTLKSG only equals unity if all s(i)s equal unity, and greater if some or all s(i)s are less than unity. However, if one considers the overall window-cum-Frost signal gain in the 'look' direction, it is given by;

$$OVRLKSG = \sum_{i=1}^{K} s(i).g(i,M) = \frac{1}{SSQ}.\sum_{i=1}^{K} s(i)^2 = 1 \quad \ldots\ldots(13)$$

where, the term s(i) multiplying g(i,M) in Eqn (13) is the pre-Frost elemental array shading coefficient. On substituting for SSQ (via Eqn (7)) it is clear that OVRLKSG equals unity. This implies that the subsequent Frost processing restores the loss in signal gain due to shading in the 'look' direction (or close to it) whilst, signals from other directions are minimised in the LMS sense. Such a selective compensation of spatial gain is not possible with the conventional beamforming approach.

3 ALGORITHM BENCHMARKS

A list of algorithm execution benchmarks summarising the capability of the hardware architecture implemented in [5] is given in table 1 below. Timings for the 20 MHz Forward Filter Path (FFP) and the 16 MHz Weight Update Path (WUP) (see, Fig.2) are presented for a variety of gain/derivative constraints and element tap combinations. Bracketed values reflect the inclusion of array shading within a given constraint combination. As before, K is the number of array elements and J is the number of taps per element.

The Benchmarks given for the constrained Frost and the Duvall LMS algorithms assume a direct mapping onto the structure shown in Fig.2. The Duvall signal 'difference' blocking is implemented in software as part of the weight update process, see [3]. The GSC algorithm is also mapped easily. However, the given GSC benchmark timings refer to the implementation of the adaptive unconstrained part of the overall GSC beamforming structure. The non-adaptive (fixed) processes are carried out separately, elsewhere, see [3 & 5]. From Table 1 it is clear that as the number of elements increases the data throughput and the filter weight update rate decreases. By introducing parallelism within the architecture in Fig.2 it is possible to counter this drop in processing rates as proposed in [3].

Real Weight/Data Vector Size	FFP		FROST (WUP) µs.				DUVALL	GSC (WUP) µs.
K x J	µs.	kHz	0 OGC		0+1 OGC		(WUP) µs.	uncnst'd Algo.
8 x 4	2.0	500	17	(20)	20	(24)	19	12
8 x 8	3.5	277	29	(36)	37	(45)	35	21
16 x 4	4.0	250	28	(35)	36	(44)	35	22
16 x 8	7.0	138	52	(67)	68	(83)	65	40
32 x 4	8.0	125	51	(66)	66	(82)	65	41
32 x 8	14.5	69	98	(128)	129	(160)	127	78

TABLE 1. Algorithm Benchmarks (In-line TMS320C30 coding assumed)

4 HARDWARE SIMULATION RESULTS

In the following scenarios a 32-element linear, equispaced, array is employed. An inter-element spacing equal to half the wavelength at the maximum signal frequency of 0.5xF(a) Hz is assumed. Where, F(a) is the array sampling frequency. All temporal frequencies are expressed normalised to F(a). The normal to the array is defined as the 'look' direction with a bearing of zero degree. Locations in the first quadrant have positive bearings and negative bearings in the second quadrant. The array mid-point has been selected as a zero phase centre. Broadband interferers were simulated using independent (uniformaly distributed) random number generators. In all cases, the spectral composition of the interferer(s) is as indicated in Fig.3, with a bandwidth equal to 20% of the centre frequency of 0.25 Hz. The level and the type of the array errors simulated, are in the form of elemental mismatches of up to ±10% in gain and ±10 degrees in phase with -20dB wideband noise (relative to the 'look' signal) at the array elements, unless stated otherwise. These levels of errors are referred to as 'moderate' array errors later on in the paper.

The Dolph Chebyshev, Ward [16], class of weighting functions is used to shade the arrays in the conventional and adaptive beamformed cases. The Dolph Chebyshev class of functions, exhibiting an equi-ripple side-lobe structure, has been employed for shading the array. Of course, other shading functions could have been employed instead, see Harris [17] for typical examples. However, the shading functions selected are designed to achieve the minimum broadening of the main-lobe response, ie. minimum loss in spatial resolution. In the case of adaptive responses a weight update rate equal to F(a) Hz for the 'Forward FIR Filter Path' (see Fig.2) is assumed, unless stated otherwise. In the simulated scenarios an octave-wide frequency band (centred on F(a)/4 Hz) was employed. An 'all-pass' Frost response was specified through the frequency constraint vector f(j) (in Eqn (10)). The beamformer weights (FF in Eqn (1)) evolve from an initial value of zero for each simulated Frost response. The values of 'µ' quoted in this paper are 32767 times smaller than usually found in the subject literature. This is a consequence of working with a 16-bit (2's complement) integer number range. Unless stated otherwise, a working value of 10^{-7} is assumed for 'µ'.

4.1 Scenarios with Interferers in the Side-lobes

A scenario with four broadband interferers and a CW pulse signal is employed. The four interferers have bearings of –66, –42, +33 & +52 degrees (corresponding to side-lobe peaks, at a signal plot frequency of F(a)/4 Hz, see [3]) while, the CW signal bearing is 5 degrees. The spectral composition of each interferer and the CW signal pulse is as outlined earlier. Each interferer is +24 dB relative to the CW signal. The resulting SINR at the array elements is –30 dB. Array imperfections, where mentioned, are of the form outlined previously.

4.1.1 Array Shading, Convergence & Coherent Cancellation Effects

A 9000-sample long by 32 elements wide input scenario is employed with the CW signal pulse existing between sample numbers 7500-9000 with moderate array errors present. The temporal unshaded 0 OGC Frost response to the

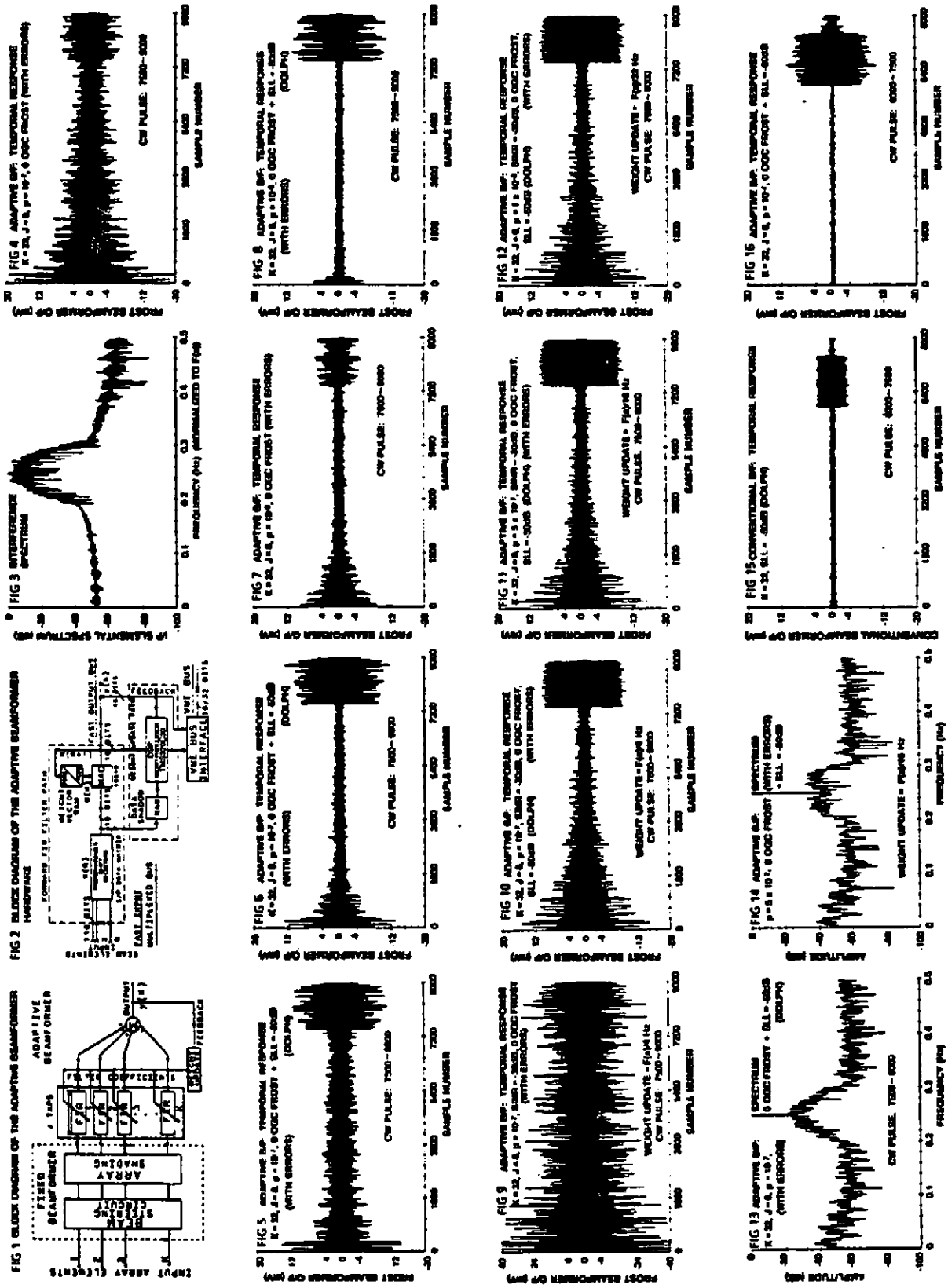

above scenario is shown in Fig.4 where J=8. The corresponding shaded 0 OGC Frost responses with SLL=-30 dB and -50 dB are shown in Figs.5 and 6, respectively. The effect of array shading within the 0 OGC) on the rate of response convergence is evident. Increasing 'μ' ten-fold enables the unshaded 0 OGC Frost response to converge faster and before the arrival of the CW pulse, compare Fig.7 with Fig.4. However, a higher 'μ' leads to increased coherent-signal-cancellation (CSC) effects over the duration of the CW pulse, see Fig.7. The corresponding shaded (SLL=-50 dB) Frost response is shown in Fig.8. The reduction in CSC effects due to array shading is also evident. The SINR of the beamformed CW pulse (relative to the output level preceding its arrival) in Fig.8 is 14.3 dB, some 4 dB higher than that in Fig.7. In spite of increased CSC effects (due to higher 'μ') the resulting SINR for the output CW pulse in Fig.8 is only 0.3 dB lower than that in Fig.6, again illustrating the beneficial effect of array shading.

The effects of array shading on adaptive beamforming in the side-lobe region is similar to that resulting from increasing 'μ' but without accentuating CSC effects. This was found to be the case, at least for a 16-element (with SLL upto –30 dB) and a 32-element (with SLL upto –70 dB) linear array employing Dolph Chebyshev shadings.

4.1.2 Array Shading & Weight Update Rate

The effect of updating filter weights at rates lower than F(a) Hz is shown in Fig.9 for a 0 OGC Frost beamformer (J=8) with its weights updated at F(a)/4 Hz in the presence of array errors. The level of the residual interference break through is high enough to conceal the CW pulse. Incorporation of (SLL=-50 dB) Dolph shading speeds up convergence, see Fig.10, and improves the output SINR by some 11 dB to 13.5 dB. Reducing the weight update rate (WUP) to F(a)/16 Hz while increasing 'μ' roughly proportionally leaves the rate of convergence unchanged (compare Fig.10 with 11). Reducing WUP further to F(a)/32 Hz while increasing 'μ' proportionally again maintains the rate of convergence, see Fig.12. Such a trade off between 'μ' and WUP broke down at WUP=F(a)/256 Hz with 'μ' equal to 100 times the starting (stated) value for the above scenario. In practice however, updating of the weights at very low rates may make beamformer response too sluggish to be useful, though this will depend on factors such as the number and composition of the interferers, their spatial velocity and their bearing relative to the 'look' direction.

It is interesting to note that updating the beamformer weights less frequently leads to reduced CSC effects, compare Fig.6 (weights updated at F(a) Hz) with Figs.10, 11 and 12 (with different 'μ' and lower WUP rates). This is due to the LMS power minimisation process becoming less sensitive to short-term correlation existing between the CW signal and the interferers. The spectral plots corresponding to Figs.6 and 11 are given in Figs.13 and 14, (resp.), which also illustrates the reduced CSC effects (compare the enhanced 0.25 Hz tonal in Fig.14 with that in Fig.13).

4.1.3 Robustness to Array Errors

The robustness of adaptive beamforming over the conventional beamformed approach is illustrated for the following three cases of array errors: a) without array errors, b) with moderate level of array errors, and c) with high levels of array errors. In the following illustrations Dolph array shading with SLL=–50 dB is used, unless stated otherwise. The performance of the shaded, 0 OGC Frost beamforming is compared with the shaded conventionally beamformed approach. The corresponding unshaded Frost responses have not been presented here since these take much longer to converge. A 8000-sample by 32 element scenario is employed (instead of 9000 samples used previously) with the CW signal pulse lasting between samples 6000 and 7500.

4.1.3.1 Absence of Array Errors

In the absence of any array errors the shaded conventionally beamformed temporal response is shown in Fig.15. The CW pulse is clearly visible with an output temporal SINR of 14 dB above the background level. The corresponding shaded 0 OGC Frost response (J=8) is shown in Fig.16 also clearly shows the CW pulse which now has an output SINR level of 16 dB. The loss in the CW signal power (due to array shading) in the shaded conventionally beamformed case is evident, compare Fig.15 with 16. Whereas, in the adaptive case this loss has been compensated for automatically in the 'look' direction, see Fig.16, (as outlined in section 2.2.1). Spectral plots, computed over the duration of the pulse and corresponding to Figs.15 and 16 are given in Figs 17 and 18, respectively. These show the enhancement of the 0.25 Hz CW tonal by the shaded conventionally beamformed approach (Fig.17) over the adaptive approach (Fig.18). With SLL=-30 dB (cf. -50dB) however, the opposite of the above was found to be true.

4.1.3.2 Moderate Array Errors

The effect of introducing moderate levels of array errors (see, section 4) in the previous scenario is considered next. Shown in Fig.19 is the shaded conventionally beamformed temporal response in the presence of moderate array errors. With an output SINR of only 2.4 dB it is difficult to detect the CW signal pulse from the background residual level. The corresponding shaded 0 OGC Frost temporal response, shown in Fig.20 yields an output SINR of 14.7 dB. Repeating the above exercise using a frequency swept FM signal (cf. CW) pulse (frequency varying

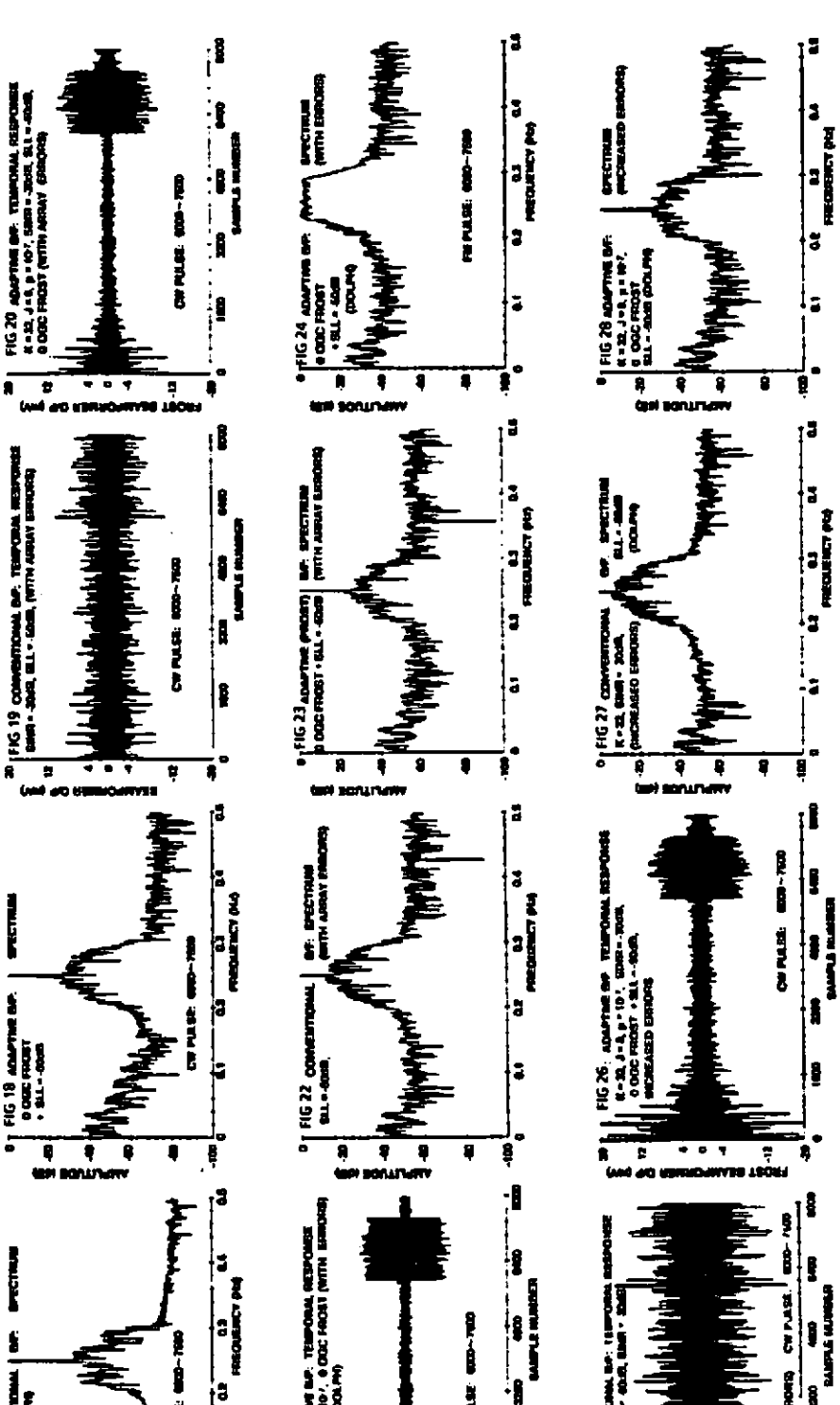

linearly by ±10% about 0.25 Hz over the 1500-sample pulse duration), Fig 21 shows the resulting shaded (0 OGC) Frost response. The frequency sweeping action lowers the short–term correlation between the FM pulse (Fig 21) and the interferers which leads to reduced CSC effects, compare with Fig.20 (CW case). Relative to the shaded conventionally beamformed response (not shown) adaptive beamforming improved the SINR of the FM pulse by some 11.4 dB. Incidentally, if the CW pulse in Fig. 20 had not been misaligned by 5 degrees to 'look' direction its output SINR would have risen by an additional 0.1 dB. This, illustrates the insignificant effect of beam steering errors on the detected signal power at low input SINRs (here, -30 dB).

Spectral plots corresponding to Figs.19 and 20 are shown in Figs.22 and 23 respectively. Adaptive beamforming has enhanced the CW tonal by some 10 dB over the corresponding conventionally beamformed approach. Repeating the above but using a SLL=-30 dB shading gave a tonal enhancement of some 17 dB. The spectral plot corresponding to Fig.21 is given in Fig.24 where, a 'flat-topped' spectrum over the FM signal band results.

4.1.3.3 With High Array Errors

The effect of higher levels of array errors (upto ±20% in gain, ±20 degrees in phase and –20 dB elemental noise) in the scenario being considered is illustrated next. Shown in Fig.25 is the shaded conventionally beamformed temporal response in the presence of higher array errors. The CW signal pulse, with a SINR of only 1 dB, is indistinguishable from the background breakthrough. Whereas, by employing a 0 OGC Frost beamforming with (SLL= -50 dB) shading raised the output detection SINR level by 11.2 dB (to 12.2 dB), see Fig.26. Spectral plots corresponding to Figs.25 and 26 are shown in Figs.27 and 28, respectively. A +20 dB spectral enhancement of the CW tonal is achieved by adaptive beamforming over the corresponding conventionally beamformed case.

From the preceding sections it is clear that the adaptive approach, unlike the shaded conventionally beamformed approach, continues to give a more robust performance especially, when increased gain and phase mismatches exist between the array elements.

4.2 Scenarios with Interferers Close to the Main-lobe

Under low SINR conditions array shading incorporated within the adaptive beamforming process results in slowing the rate of removal of interferers residing close to the array main-lobe. The rate of nulling depends on the extent of broadening of the mainlobe which in turn depends on the array shading parameter, SLL. For example, consider the case of a +30 dB broadband interferer at bearing 5 degrees. A 0 OGC Frost beamformer (J=8) took twenty times longer (some 180,000 sampling intervals) to converge when employing a SLL=–30dB Dolph shading than its unshaded counterpart. With a SLL=-50 dB shading, the convergence time was closer to 50 times longer than without shading. Such a 'sluggish' response might even be considered desirable in some high SINR sonar applications. By being more tolerant to strong but misaligned signals the (shaded) adaptive beamformer behaves more like a conventional beamformer close to the main-lobe region. In the array side-lobes however, the performance of the beamformer benefits from array shading as demonstrated earlier on.

4.3 Broadband 'Spatial' Response

In order to get an overall comparison between adaptive and conventional beamforming approaches a +0 dB broadband interferer was swept spatially from -90 to +90 degrees about a -30 dB CW pulsed signal, bearing 0 degree, (both sources centred at F(a)/4 Hz). The 1000-sample CW signal pulse was generated after some 3000 initial sampling intervals had elapsed (for convergence to occur) for a given interferer bearing. Moderate levels of gain and phase mismatches and noise at the array elements (see, section 4) were also simulated. The output SINR for the CW signal pulse versus interferer bearing was plotted (not shown) at one degree intervals for the conventionally beamformed cases (with SLL = –30 dB and –50 dB array shading) and also for the shaded and unshaded adaptive cases.

It was found that Frost beamforming, relative to the conventionally (shaded) beamforming, lowered the pulse detection threshold level by between 10 and 15 dB in the side-lobe regions. A 32-element (0+1) OGC Frost algorithm (J=8) was employed. The incorporation of array shading within the Frost process smooths out variations in SINR in the side-lobes while broadening the main-lobe response, somewhat. For higher input SINR values (eg. –20 dB..–10dB..0dB) adaptive beamforming enhanced signal detectability by approximately 15 dB over the conventional approach for bearings greater than 10 degrees about the 0 degree 'look' direction. For longer arrays (e.g. 128 elements) enhanced signal detectability is still achievable but to a reduced extent.

5 CONCLUSIONS

The simulated hardware performance of a 16-bit adaptive beamformer with 32 elements, each up to 8 taps deep, has been demonstrated. The benefits of adaptive beamforming over the conventional approach have been demonstrated for a linear, medium sized equi-spaced element array. The LMS based Frost/GSC adaptive beamforming technique gives a robust performance in the presence of multiple broadband interferers and realistic levels of hydrophone mismatch and noise. For a 32-element linear array adaptive beamforming, relative to conventional beamforming, enhanced the detectability of weak (-30 dB) 'look' signals in the presence of a broadband interferer residing in the array side-lobes by between 10 – 15 dB.

The incorporation of Dolph array shading within the adaptive gain constraints is shown to aid in signal detection by mitigating the leakage of strong broadband interferers residing in the array side-lobes. The main benefits of array shading are reduced coherent-signal-cancellation effects and increased rates of convergence, the latter allowing beamformer weights to be updated at rates lower than the array sampling frequency. For strong interferers residing close to the main-lobe array shading reduces the rate of their removal due to a broader initial main-lobe response. For low SINR applications a Frost-GSC algorithm employing a simple zero – order gain constraint is adequate for detecting weak (up to -40 dB) and misaligned (by 5 degrees) signals about the 'look' direction with realistic levels of errors present at the array elements. The use of higher order (derivative) gain constraints is mainly required when operating in high SINR scenarios. Algorithm execution benchmarks for the architecture implemented in hardware have been presented for a number of adaptive approaches incorporating a combination of array shading and 'look' gain constraints.

6 ACKNOWLEDGEMENTS

This work was funded under the Private Venture (PV) Research Programme by Marconi Underwater Systems Ltd., (MUSL), Waterlooville, Portsmouth. The author expresses his gratitude to the Technical Directorate of the Marconi Company for permitting to publish this paper. The efforts and helpful suggestions made by P J Hutchings and P R Openshaw (both of MUSL, Waterlooville) and D C Atmore and S A N Whitehead (both of MUSL, Templecombe) during the preparation of this paper are also gratefully acknowledged by the author.

7 REFERENCES

[1] A A WINDER, "Underwater Sound - A Review: II Sonar System Technology", IEEE Trans Sonics and Ultrason, Vol. SU 22(5), p291, Sept. 1975.

[2] A C SMITH, G C L SEARLE, "Empirical Observation of a Sonar Adaptive Array", IEE Proc. F, Commun. Radar & Signal Processing, Vol. 132(7), p595, 1985.

[3] M TRIVEDI & D C ATMORE, "Real-Time Adaptive Processing of Broadband Sonar Signals on a Single-Card with High Data Throughput Rates", Proc. UDT Conference, Paris, p1124-1133, Microwave Exhibition and Publishers Ltd., April 1991.

[4] K M BUCKLEY & L J GRIFFITHS, "An Adaptive Generalized Sidelobe Canceller with Derivative Constraints", IEEE Trans. Antennas and Propogation, vol. AP-34, No. 3, p311-319, March 1986.

[5] M TRIVEDI, D C ATMORE & C H STARKIE, " A Versatile Adaptive Digital Sonar Beamformer", Proc. I.O.A. Vol. 11, Part 8, p228-237, Dec. 1989.

[6] O L FROST, III, "An Algorithm for Linearly Constrained Adaptive Array Processing", IEEE Proc., Vol. 60(8), p926, Aug. '72.

[7] J E HUDSON, "Adaptive Array Processing", Pub.: IEE, London & New York, Peter Peregrinus Ltd., 1981.

[8] M H ER & A CANTONI, " Derivative Constraints for BroadBand Element Space Antenna Processors", IEEE Trans. Acoustics, Speech and Signal Processing, vol. ASSP-31, No. 6, p1378-1393, Dec. 1983.

[9] H COX, R M ZESKIND & M M OWEN, "Robust Adaptive Beamforming", IEEE Trans. on Acoustics, Speech & Signal Processing, Vol. ASSP-35, p1365-1376, Oct. 1987.

[10] K M DUVALL, "Signal Cancellation in Adaptive Antennas: The Phenomenon and a Remedy", Ph.D Thesis, Stanford Univ., USA, 1983.

[11] Y L SU, T J SHAN & B WIDROW, "Parallel Spatial Processing: A Cure for Signal Cancellation in Adaptive Arrays", IEEE Trans. on Antennas and Propogation, vol. AP-34, p347-355, March 1986.

[12] T J SHAN & T KAILATH, "Adaptive Beamforming for Coherent Signals and Interference", Proc. II IEEE Workshop on Spectral Estimation, Tampa, FL., Nov 1983.

[13] T J SHAN & T KAILATH, "Adaptive Beamforming for Coherent Signals and Interference", IEEE Trans. Acoust., Speech, Signal Process., vol. ASSP-33, No. 3, p527-536, June 1985.

[14] J H LEE & J F WU, "Adaptive Beam forming without Signal Cancellation in the presence of Coherent Jammers", IEE Proc., vol. 136, Pt. F, No. 4, p169-173, Aug. 1989.

[15] P BRAGARD & G JOURDAIN, "A fast self-optimised LMS algorithm for non-stationary identification – application to underwater equalization", IEEE ICASSP Conf., Vol. D5.11, pp. 1425-28, 1990.

[16] H R WARD, "Properties of Dolph-Chebyshev weighting functions", IEEE Trans., AES-9, p785-786, 1973.

[17] F J HARRIS, "On the Use of Windows for Harmonic Analysis with the Discrete Fourier Transform", Proc. IEEE, No. 66, p51-83, 1978.